CORE
Metadata, citation and similar papers at core.ac.uk
Provided by Central Archive at the University of Reading

JOURNAL OF GEOPHYSICAL RESEARCH, VOL. 116, D18111, doi:10.1029/2011JD016206, 2011

Changes in water vapor transports of the ascending branch of the tropical circulation

Matthias Zahn[1] and Richard P. Allan[2]

Received 4 May 2011; revised 1 July 2011; accepted 13 July 2011; published 24 September 2011.

[1] Recent studies have found contradicting results on whether tropical atmospheric circulation (TAC) has intensified or weakened in recent decades. Here we reinvestigate recent changes in TAC derived from moisture transports into the tropics using high temporal and spatial resolution reanalyses from ERA-Interim. We found a significant strengthening of both the lower-level inward transports and the midlevel outward transports over the recent two decades. However, the signal in the total budget is weak because the strengthening of the inflow and the strengthening of the outflow neutralize each other, at least to some extent. We found atmospheric humidity to be relatively stable, so we suggest that the intensification is mainly caused by an intensification of the wind-related circulation strength. The exact quantitative values were found to depend heavily on whether the calculations are based on mean or instantaneous values. We highlight the importance of using the instantaneous values for transport calculations, as they represent the coincidence of high wind speeds and high atmospheric humidity.

Citation: Zahn, M., and R. P. Allan (2011), Changes in water vapor transports of the ascending branch of the tropical circulation, *J. Geophys. Res.*, *116*, D18111, doi:10.1029/2011JD016206.

1. Introduction

[2] Recent and future changes in the statistical characteristics of the tropical atmospheric circulation (TAC) pattern and associated changes in the tropical hydrological cycle do not only locally affect the weather properties in the tropical areas but they have an influence on the extratropical regions. The general TAC pattern consists of convective regions of upward, ascending air movement (ASC) and of regions of downward, descending air motion (DESC), with low-level flow into ASC and midlevel outflow into DESC commonly referred to as the Hadley Cell circulation. Along with the upward air motion, ASC contains most of the tropical precipitation and in its annual cycle by and large follows the Sun's zenith. Part of the water vapor originates from evaporation in areas close by, but additionally large amounts of water are transported by atmospheric movements from DESC, causing a largely positive tropical water balance (precipitation-evaporation) at the cost of the dry subtropics. A number of recent studies have addressed past and possible future changes in the moisture budget or in other components of the hydrological cycle over the tropics or over parts of the tropics. An increase in low-level atmospheric water vapor of 7% per degree of warming is derived from theoretical considerations (Clausius-Clapeyron relation, e.g., *Wentz and Schabel* [2000]; *Trenberth et al.* [2003]; *Held and Soden* [2006]; *O'Gorman and Muller* [2010]). A straightforward assumption is a proportional increase in precipitation and evaporation as well.

[3] However, reality seems to be more complicated, and precipitation (P) and evaporation (E) changes have not been found to be equally distributed in space, time, and intensity and may be constrained by the tropospheric energy budget [*Allen and Ingram*, 2002]. *Allan and Soden* [2008] find an amplification of P mainly in the higher-percentile bins, meaning that the intensity of extreme P events in particular may increase with global warming. Also, *Chou et al.* [2007] found a P increase to induce wetter wet seasons but found the dry seasons to become slightly drier as the atmosphere warms.

[4] Looking at precipitation trends, *Allan and Soden* [2007] and *Allan et al.* [2010] find large discrepancies between model and observation data. They distinguish between ASC and DESC by using monthly mean 500 hPa vertical wind motion from reanalysis data. *John et al.* [2009] define their ASC and DESC similarly, concluding that the tendency of ASC to become wetter and DESC to become dryer is robust over models and satellite observations. A very detailed study on changes in the hydrological cycle has been undertaken by *Seager et al.* [2010]. They break down changes in the moisture budget into thermodynamically and dynamically induced changes using daily model mean values and find the thermodynamic part to increase P-E through increasing specific humidity, while a weakening of the circulation opposes this trend. Using monthly mean sea level pressure data, *Vecchi et al.* [2006] also find a weakening of the tropical circulation, and *Power and Smith* [2007] find a weakening of atmospheric circulation indices over the

[1]Environmental Systems Science Centre, University of Reading, Reading, UK.
[2]Department of Meteorology, University of Reading, Reading, UK.

Copyright 2011 by the American Geophysical Union.
0148-0227/11/2011JD016206

Pacific. Similarly, *Gastineau and Soden* [2011] identified a weakening of recent surface wind extremes. *Harrison* [1989], in an earlier study using observed surface winds, finds no statistically significant trend, at least for the tropical Pacific. This is in contrast to other studies, older and more recent ones, that find a strengthening in the tropical circulation, e.g., those by *Whysall et al.* [1987] and *Bigg* [2006], who both find a strengthening of the surface trade winds.

[5] *Sohn et al.* [2004] compiled a global data set of moisture divergence and convergence by merging satellite and reanalysis data, which *Sohn and Park* [2010] later use to investigate changes in tropical circulation and related moisture transports. *Sohn and Park* [2010] find a strengthening of the tropical circulations over the past decades. *Mitas and Clement* [2005] find a strengthening of the Hadley Cell circulation in its northern branch using two coarse-resolution reanalysis data sets, ERA-40 [*Uppala et al.*, 2005] and National Centers for Environmental Prediction's NCEP-1 [*Kalnay et al.*, 1996]. They define intensity as the maximum in the December-January–February–averaged stream function between 0°N and 30°N, and *Lu et al.* [2007], in the Intergovernmental Panel on Climate Change (IPCC) AR-4 model data, find the Hadley Cell expanding in response to increasing subtropical static stability. Their Hadley Cell definition is based on annual means of ω at 500 hPa.

[6] All these studies and their sometimes opposite results highlight the importance of continuing to investigate the changes in tropical circulation, especially as they are crucial for understanding changes in the P-E budget and for understanding changes in water vapor transports. Especially in the tropical regions, most of the precipitation does not originate from nearby evaporation (e.g., see recycling ratio by *Trenberth et al.* [2003]).

[7] We thus here reinvestigate the water vapor transports into the ascending regions of the tropics by applying a high-resolution reanalysis data set. Unlike the methods in most of the above mentioned studies, we base our investigations not only on the time mean values but also on high-resolution data of the six-hourly output fields. We will thereby highlight the importance of using instantaneous and vertically resolved values for moisture transport calculations.

2. Data

[8] We calculate atmospheric moisture transports using horizontal and vertical wind components, pressure, and atmospheric humidity of the lowest 31 model levels from a recent reanalysis, the European Centre for Medium-Range Weather Forecasts (ECMWF) ERA-Interim [*Simmons et al.*, 2007; *Dee and Uppala*, 2009; *Dee et al.*, 2011] for the period 1989–2008. The data are available at a horizontal resolution of 0.7°. From ERA-Interim horizontal and vertical wind vectors (**U**, **V**, and ω), specific humidity (q) and vertical pressure information were used between ±30° latitude, representing the tropics. Calculations were restricted to the lowest 31 model levels (representing the atmosphere up to an altitude of ~200 hPa), which contain almost all of the atmospheric moisture. Additionally, precipitation (P) and evaporation (E) were used as a reference to confirm resulting moisture budgets.

[9] Coarse resolution reanalysis data (e.g., ERA-40 or NCEP) have been found to suffer from some insufficiencies in the hydrological cycle. For instance, *Trenberth et al.* [2005] find differences in column-integrated atmospheric water vapor between satellite observations and coarse-resolution reanalysis data. In the presatellite era a problem of mass conservation associated with the data assimilation in ERA-40 existed. The ERA-Interim reanalysis has especially been designed to overcome these issues in the hydrological cycle (*Dee and Uppala* [2009]). We will also show that ERA-Interim moisture budgets from transports are on the same level as the P-E budget. We thus believe that the 4-D high-resolution data are adequate for our study of the hydrological cycle. As will become evident in the section 3, high temporal and spatial resolution, horizontally as well as vertically, large data coverage, and homogeneity are crucial to the methodology in our study. These criteria, central to our study, are so far only met by reanalysis data.

3. Methodology

[10] Most of the studies mentioned in section 1 investigate changes in the tropical moisture budget by means of average variables, for defining ASC and DESC as well as for calculating the moisture transports. However, the spatial distribution of the ASC and DESC regions of the Hadley circulation roughly consisting of one ASC along the equator and DESC north and south is a rather theoretical construct to describe the mean circulation and usually is not representative of the instantaneous fields. The instantaneous fields are characterized by numerous individual convective cells and convective regions, irregularly distributed over the tropics (e.g., Figure 1). We take advantage of the high temporal and spatial resolution of ERA-Interim and use ASC and DESC not only defined in the conventional way by applying mean fields but also using instantaneous variables. With the latter, we hope to resolve individual convective cells or regions much better and more realistically compared to just using means. We herewith also resolve more accurately the complex vertical structure of the tropical circulation, consisting of lower-level flow toward the regions of convection and vice versa in the midlevels.

[11] Our calculations are subdivided into two steps:

[12] 1. ASC, DESC, and the boundary separating ASC from DESC are identified.

[13] 2. The transport of water vapor over this boundary is calculated.

[14] Both steps are described individually in sections 3.1 and 3.2. Trends in section 4 will be calculated by a least squares fit, and significance will be tested by a *t* test based on the respective annual means.

3.1. Defining Ascending and Descending Branches of the Tropical Atmospheric Circulation

[15] In the classical view on the tropical circulation, convection and convergence at the intertropical convergence zone (ITCZ) drive a wind flow pattern consisting of the moisture-laden trade winds, which carry water vapor into the equatorial tropics at the lower levels, and a poleward directed flow at the midlevels. However, such simplification is only valid for the mean circulation and can be more complex in the instantaneous fields; that is, sinking air

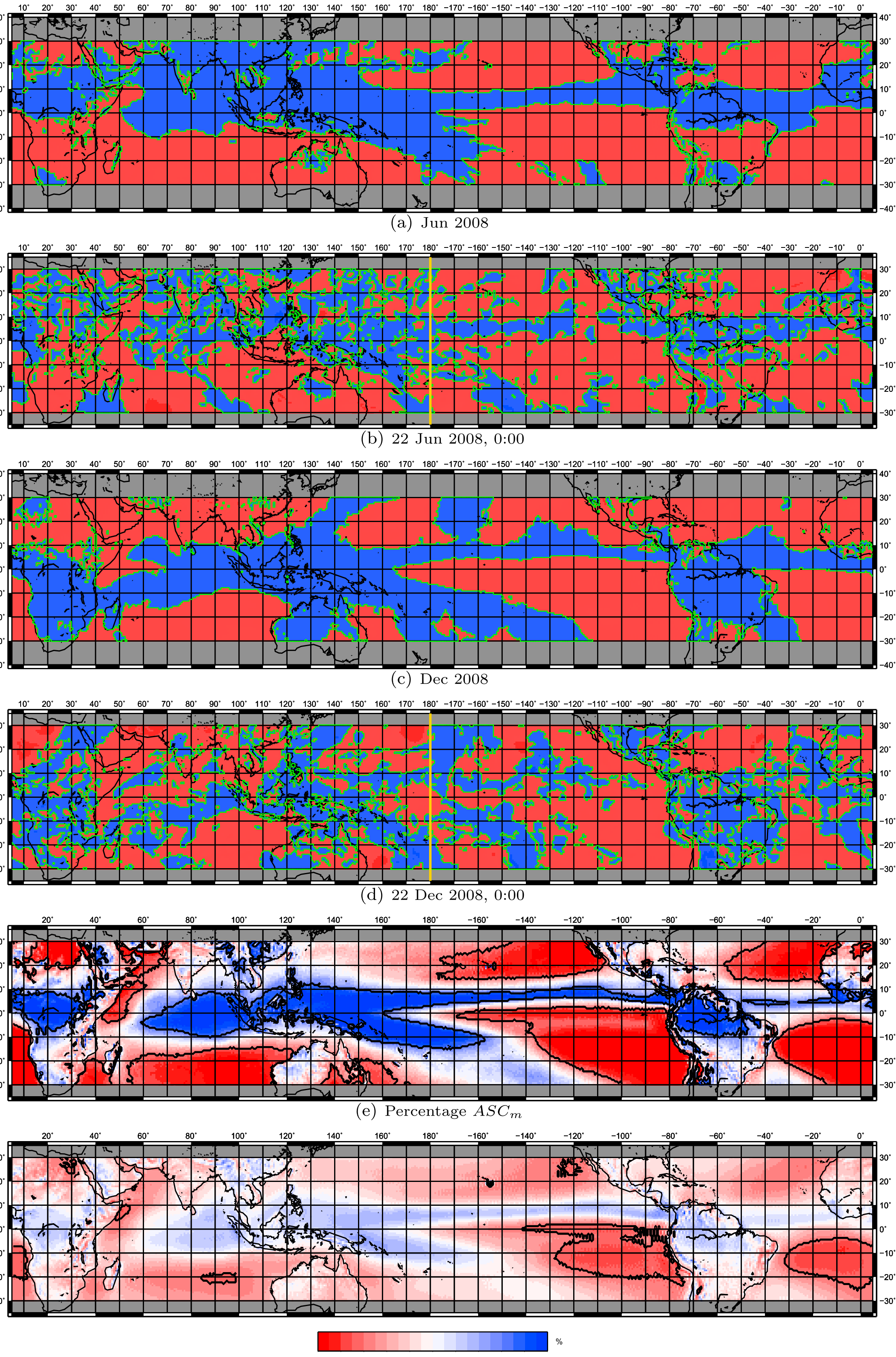

(a) Jun 2008

(b) 22 Jun 2008, 0:00

(c) Dec 2008

(d) 22 Dec 2008, 0:00

(e) Percentage ASC_m

(f) Percentage ASC_i

Figure 1

Table 1. Acronyms for the Different Experiments

ASC and DESC Based on	MT Based on Monthly Mean Variables	MT Based on Six-Hourly Instantaneous Variables
Monthly mean ω	MT_{mm}	MT_{im}
Six-hourly instantaneous ω	MT_{mi}	MT_{ii}

motions can take place within the tropics right next to convective cells and can thus circulate for a while within the tropics before being shifted away.

[16] To take into account these more complex circulations, we not only base our investigations on mean fields but, unlike other studies, we also apply quasi-instantaneous ones. This holds not only for the usage of the wind vectors and humidity values applied but also for the definition of the ASC and DESC masks.

[17] To estimate ASC and DESC, we vertically averaged vertical wind (ω) over each grid cell. When averaging, ω at each vertical level was weighted by the level's pressure depth. Grid cells with upward total ω are recorded as ASC; regions with downward total ω are recorded as DESC. We used two different ASC and DESC masks, one based on monthly mean values for ω (ASC_m), resulting in 240 different masks (20 × 12, one per month) and another one based on instantaneous ω (ASC_i), resulting in 29,220 masks (one for each time step). Using instantaneous ω enables us to investigate the moisture budget of highly dynamical regimes rather than fixed geographic regions.

[18] Examples of both ways of defining ASC and DESC are presented in Figure 1. The two examples derived from the monthly means (Figures 1a and 1c) closely resemble the uniform pattern of the Hadley Cell, with upward wind motion at the ITCZ and downward wind motions north and south. The ITCZ is located a bit north/south following the respective zenith of the Sun.

[19] In the instantaneous masks for ASC and DESC, the situation appears more complicated: unlike in the mean fields, several individual cells of ASC_i are irregularly distributed all over the area. There is a low resemblance between instantaneous ASC_i and mean ASC_m masks, which may have implications when calculating the moisture transports. For instance, the instantaneous ASC_i masks cover large regions which on average would belong to DESC and vice versa. While the locations of ASC_m are relatively constant over the year (denoted by thick colors in Figure 1e), the thinner colors in Figure 1f indicate the high variability of ASC_i. Only a few regions in the subtropical oceans belong to $DESC_i$ more that 80% of the time. Note that we will use the terms ASC and DESC for all regions of rising and sinking air in both the mean and the instantaneous fields, although ASC and DESC are usually used for only two centers of the tropical circulation.

3.2. Estimation of the Moisture Budget

[20] Calculating moisture transports relates wind vectors with atmospheric moisture content. To estimate the moisture budget, the moisture transport (MT) is calculated along all the n_b boundary segments b between ASC and DESC (green lines in Figure 1). Therefore, the perpendicular wind vector (WP, positive toward ASC) and the precipitable water content (PWC) are estimated along each boundary segment on each of the n_l vertical model levels l. For each segment on each level, MT then is the product of WP and PWC. The total net moisture budget at time t then is the sum of MT at each segment on each level:

$$MT_t = \sum_{b}^{n_b} \sum_{l}^{n_l} WP_{bl} \cdot PWC_{bl}. \quad (1)$$

[21] This moisture budget is calculated in two ways: on the basis of monthly average values for specific humidity (q) and zonal and meridional wind U and V (m = mean variables) on the one hand as well as on the basis of (six-hourly) instantaneous values (i = instantaneous variables) on the other. Instantaneous as well as monthly average values are applied to the monthly mean (m = mean mask) ASC and DESC masks as well as to the instantaneous mask (i), leading to four different experiments for the moisture transport. Throughout this paper, the different experiments will be referred to by the acronyms listed in Table 1. Here the first subscript refers to the variables used to calculate the transports, and the second subscript refers to the mean or instantaneous ω to estimate the mask.

[22] Additionally, six-hourly accumulated precipitation and evaporation values are used for all ASC grid boxes, and the moisture budget is estimated from P-E.

4. Results

[23] Here the results of applying the moisture transport calculations of the four experiments are described and compared to each other. This is first done on the basis of absolute values and then on the basis of relative values, MT per m along the boundary; then the vertical profile is examined and, finally, trends in the lower-level inflow and in the midlevel outflow are analyzed separately.

4.1. Absolute Moisture Budgets

[24] Presented in Figure 2 are the time series and annual cycle of the absolute net moisture transport into ASC on the basis of all the instantaneous-mean variable combinations. Also added is the P-E budget, but only for ASC_m. A large spread in the absolute mean budgets is evident, with the annual mean ranging from as low as 193 $km^3\ d^{-1}$ in MT_{mi} to as high as 651 $km^3\ d^{-1}$ in MT_{ii} (Table 2). One reason for the discrepancies may be the different sizes and locations of the

Figure 1. Examples of patterns of ASC and DESC from mean and instantaneous vertical wind. Regions of upward (blue) and downward (red) vertical wind motion and the boundary separating both (green lines) are shown based on (a) mean ω in June 2008; (b) instantaneous ω at 00:00 UT, 22 June 2008; (c) mean ω in December 2008; and (d) instantaneous ω at 00:00 UT, 22 December 2008. Yellow vertical lines mark longitude of the Sun's zenith in instantaneous maps. Percentage of time steps a grid box belongs (e) to ASC_m and (f) to ASC_i. Black lines enclose regions belonging to ASC for less than 20% to more than 80% of the time.

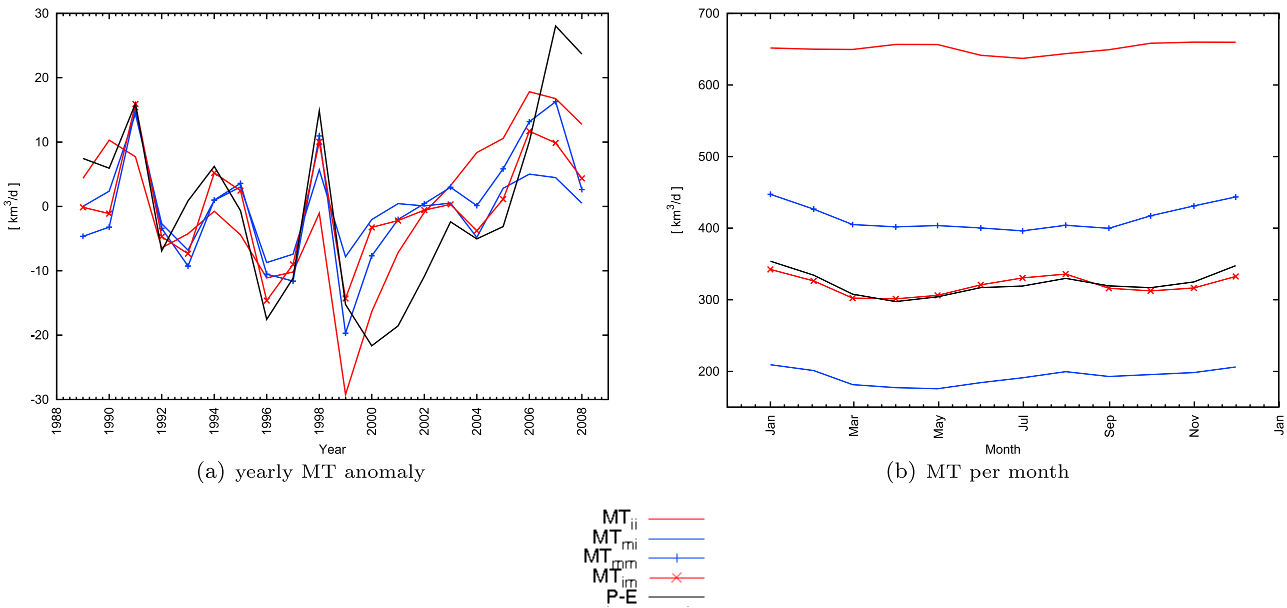

Figure 2. Absolute net water transport into ASC and precipitation-evaporation balance. (a) Time series of yearly anomaly. (b) Monthly means. Red (blue) lines indicate estimation based on instantaneous (monthly) mean wind and humidity. Solid (crossed) lines indicate ASC mask on the basis of instantaneous (monthly) mean ω. Black line is precipitation-evaporation balance for ASC-based monthly mean ω.

base areas, depending on whether ASC is gained from instantaneous or mean ω (Figure 3). The reason for differences between the MT_{im} and MT_{mm} (MT_{ii} and MT_{mi}), both using the same base region ASC_m (ASC_i), is not so obvious, and one would think that the averaging procedure would not affect the results that much. Indeed, many studies used means of variables for such budget studies. A caveat in averaging ω is that upward and downward ω are not normally distributed around zero. This has implications for the definition of the ASC. Over the tropics there seems to be a tendency of a small fraction of grid cells with extensive upward ω, whereas a larger fraction of grid cells are characterized by downward vertical wind of lower magnitude. In reality, these are the tropical convective cells and the area of weak sinking motions. In ASC_m a grid cell, which is passed by only a couple of strong convective cells, could thus be assigned to ASC_m, although belonging to the region of DESC most of the time. The difference between the budgets of the same regions is discussed in section 4.3, where we look closer at the vertical profile of transports.

[25] Despite the difference in base area size and in the mean absolute budget, the time series and annual cycle show no systematic differences in their statistical properties: they all take similar courses, i.e., they are peaking at around 1991 and in the El Niño year 1998 and have a minimum at around the La Niña year 1999. Correlation coefficients are higher than $r = 0.6$. Also, all graphs share a moderate yearly and monthly variability (standard deviations are between $\sigma = 5$ and $\sigma = 15$) and they all have positive, but insignificant, trends. Only in MT_{mm} is a statistically significant trend found, but on a relatively low confidence level. The slight increase cannot be explained by a change in base area size of ASC, which is in fact slightly decreasing (not shown). The temporal evolution of the yearly mean size of the base areas of ASC_m and ASC_i is shown in Figure 3a. The area of ASC_m is 10% larger, and its size has higher yearly variability. Owing to the fragmentation into many small areas of ASC_i and in contrast to its smaller size, the boundary around ASC_i is twice as long as the one around ASC_m (Figure 3b).

[26] Moisture fluxes over static boundaries have successfully been calculated before, e.g., for the polar regions studied by *Bengtsson et al.* [2011], who compared the moisture transport budget with P-E in their area. To estimate the validity of our calculations, we also compared our transport budgets with P-E over ASC_m. The relationship between P-E and atmospheric moisture transports for a given region and time period is

$$MT_{in} - MT_{out} = P - E + \Delta PWC, \qquad (2)$$

with MT_{in} (MT_{out}) being the moisture transport into (out of) (passing the boundary) the region, P and E being the precipitation and evaporation, and ΔPWC being the change of atmospheric water content over the region. Assuming rela-

Table 2. Statistical Values for Time Series of Yearly Absolute Mean Net Moisture Budget[a]

Acronym	Mean ($km^3\ d^{-1}$)	σ ($km^3\ d^{-1}$)	Trend (($km^3\ d^{-1}$) yr^{-1})	Significance Level of Trend
MT_{ii}	651.1	11.74	0.612	ns 0.9
MT_{im}	320.3	8.11	0.236	ns 0.9
MT_{mm}	404.6	9.39	0.514	s 0.9, ns 0.95
MT_{mi}	192.7	5.53	0.017	ns 0.9
P-E in ASC_m	320.0	14.03	0.274	ns 0.9

[a]See Figure 2. Acronym, acronym of experiment; mean, average over investigation period (1989–2008); σ, standard deviation of annual means; trend, trend of annual mean (as calculated by a least squares fit); and significance level of trend, level at which trend is significant (s) and/or no longer significant (ns). Statistical significance is tested according to a *t* test based on the yearly numbers.

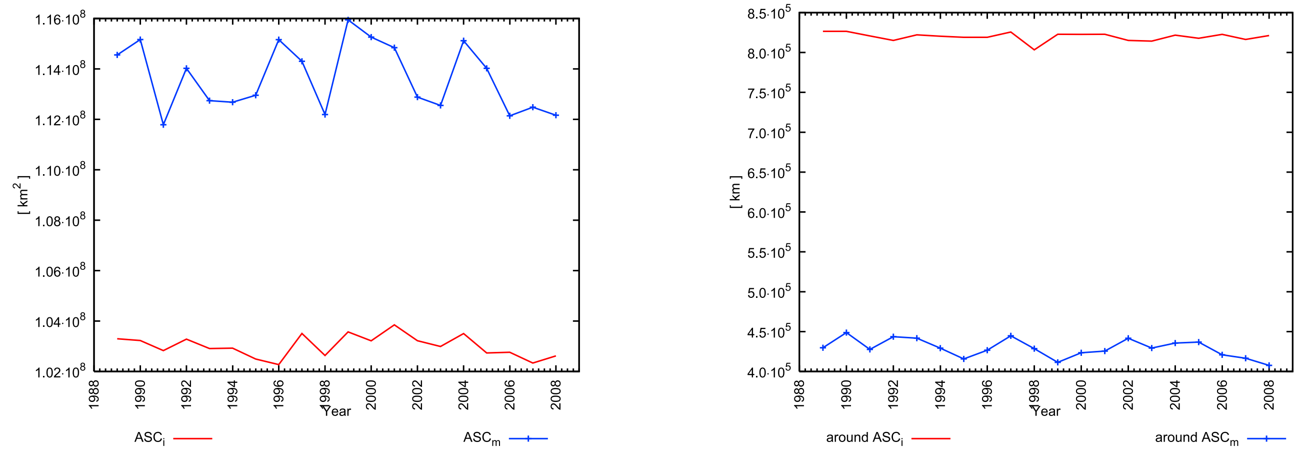

(a) area of ASC per year (b) boundary length per year

Figure 3. Area size of and boundary length around ascending regions. Yearly time series of (a) the area size of ASC$_i$ and ASC$_m$ and (b) the length of the boundary line around ASC$_i$ and ASC$_m$.

tively small changes in PWC, we use the relationship $MT_{in} - MT_{out} \sim P - E$ to compare both budgets.

[27] P-E over ASC$_m$ is given as a black line in Figure 2. The ω, wind, and humidity are calculated on a time step of 30 min in ERA-Interim, which we assume to be instantaneous. P and E in ERA-Interim are given as six-hourly accumulated values. The individual convective cells are moving too fast, or, in other words, the instantaneous masks for ASC are highly variable, even from one time step to the next 6 h later. This inhibits the use of accumulated P and E values for the instantaneous ASC. Consequently, it was only possible to estimate P-E over the relatively steady areas of ASC$_m$. Instantaneous P and E on a temporal resolution of 30 min would also be needed for balancing equation (2), which are not available to us. Please note that as a consequence of the four times daily instantaneous values, we do not have a continuous integration of instantaneous moisture flux but rather a set of four observations per day.

[28] Among the two absolute net moisture transport estimates for ASC$_m$, only the one based on instantaneous variables is close to the P-E balance. MT$_{mm}$ is about 100 km^3 d^{-1}, or about 25% too high, and only the yearly time series share similar properties (same course, maxima and minima). In the annual cycle, two maxima are evident in the transport budget of MT$_{im}$ and of P-E, in December–January and July–August, whereas the July–August peak is missing in MT$_{mm}$.

[29] We conclude at this point that a huge quantitative spread in the absolute amount of the moisture budgets is evident, depending on whether mean or instantaneous values are applied to generate ASC or to calculate the transport. Comparison with P-E reveals a close similarity to the instantaneous value-based calculations, suggesting that our moisture flux calculations are principally realistic. There are also differences in the size of the area between ASC$_m$ and ASC$_i$, which inhibit direct comparisons of absolute budgets and also highlight the necessity to investigate the influence of the size of the area.

4.2. Water Vapor Flux Over Boundaries

[30] In section 4.1, absolute transports into ASC$_m$ and ASC$_i$ were lacking comparability because of differently sized base areas. For a more straightforward comparison, we calculate the net horizontal transports per meter across the boundary separating DESC and ASC (denoted by green lines in Figure 1). The resulting unit independent of the area size is mass of water per second and meter across the boundary (kg m^{-1} s^{-1}). Their time series are shown in Figure 4, and some statistical quantities are listed in Table 3.

[31] Using instantaneous wind and humidity results in transport budgets of similar magnitude (see red lines in Figure 4a), regardless of whether ASC$_m$ or ASC$_i$ are applied. However, the budget for ASC$_i$ is consistently a bit higher and exhibits lower year-to-year variance. We find an offset in the MT$_{mm}$ transport budget, which is about 20% higher, and much lower values are found in MT$_{mi}$.

[32] There is a surprising difference between transports into ASC$_m$ and ASC$_i$. Normally, averaging would be expected to reduce variability. However, here we find twice as high numbers in annual variability for the yearly budget of ASC$_m$. The yearly amount of transports into ASC$_m$ (MT$_{im}$ and MT$_{mm}$) is extremely highly correlated (r = 0.98).

[33] Also, for these unified transports, all time series share a positive trend. This trend is negligible and insignificant for MT$_{mi}$. Trends of annual net transports are statistically significant at the 90% level for the instantaneous variables in experiments MT$_{im}$ and MT$_{ii}$. Here relative to a similar mean, the trend is twice as large for MT$_{im}$. The most pronounced trend is evident in MT$_{mm}$, when only mean variables are applied. At the 95% level it has the highest statistical significance of the four experiments.

[34] We find a systematic difference in the annual cycle between calculating the transports from the instantaneous variables and the mean variables. In Figure 4b the solid lines denoting the transports per month into ASC$_i$ do not show any significant differences over the year. For the net transports into ASC$_m$, however, there are two maxima at solstice times, in boreal and austral summer, and minima at equinox times. Over the entire tropics (±30° latitude, DESC and ASC), we found a weak annual cycle for the P-E budget, with only one minimum in boreal summer. We believe that this could be explained by the unequally distributed land masses along the latitudes. A higher fraction of land alters

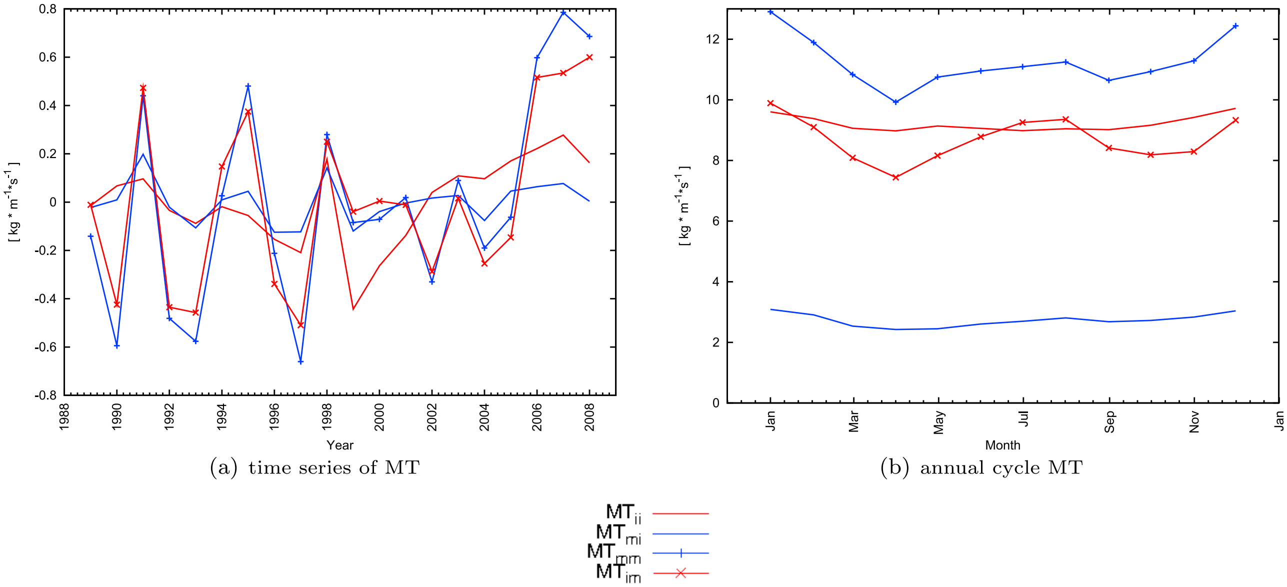

Figure 4. Net moisture transport over boundary into ASC. (a) Anomaly of annual net transport of water vapor across boundary separating DESC and ASC in kg m^{-1} s^{-1}. (b) Annual cycle of transport of water across boundary separating DESC and ASC in kg m^{-1} s^{-1}. Solid (crossed) lines denote ASC defined from instantaneous (monthly) mean ω, red (blue) lines denotes instantaneous (monthly) mean humidity and wind used for calculating the transport.

the physical properties, increases average surface temperatures in boreal summer, and thus enhances E, causing these minima in the budget (maximum in the outflow). The one peak annual cycle in MT_{ii} is slightly visible, with the highest value of 9.72 kg m^{-1} s^{-1} in December and the lowest value of 8.98 kg m^{-1} s^{-1} in April and July. We conclude that the two minima per year are an artifact of averaging ω when identifying ASC and highlight the importance of using the instantaneous values.

4.3. Vertical Profile of Moisture Transports

[35] In many studies, the moisture transports are looked at as net transport budgets and idealized as vertical means or approximated using wind vectors at a particular level (see section 1). This especially is the case when satellite data are applied because such data usually are available for the lower levels only or for the totality of the atmosphere. However, the situation in reality is more complicated, especially as the vertical profile consists of an inflow at the lower level and an outflow at the midlevels. Thus, changes in the water budget in ASC can either be influenced by changing wind characteristics at the lower inflow levels or by changing wind characteristics at the outflow levels above. Further, in a constant wind regime, the ASC moisture budget may change because of changing atmospheric humidity either at the lower level or at the midlevels.

[36] A more comprehensive picture of the vertical inflow and outflow pattern is shown in Figure 5. All the experiments show a vertical pattern consistent with the Hadley circulation, a moisture inflow at the lower levels, and an

Table 3. Statistical Values for Time Series of Yearly Net Moisture Transport Per m[a]

Acronym	Mean (kg m^{-1} s^{-1})	σ (kg m^{-1} s^{-1})	Trend ((kg m^{-1} s^{-1}) yr^{-1})	Significance Level of Trend
MT_{ii}	9.21	0.18	0.011	s 0.90, ns 0.95
MT_{im}	8.69	0.36	0.024	s 0.90, ns 0.95
MT_{mm}	10.97	0.43	0.037	s 0.95, ns 0.99
MT_{mi}	2.73	0.09	0.001	ns 0.90

[a]See Figure 4. Acronym, acronym of experiment; mean, average over investigation period (1989–2008); σ, standard deviation of annual means; trend, trend of annual mean (as calculated by a least squares fit); and significance level of trend, level at which trend is significant (s) and/or no longer significant (ns). Statistical significance is tested according to a t test based on the yearly numbers.

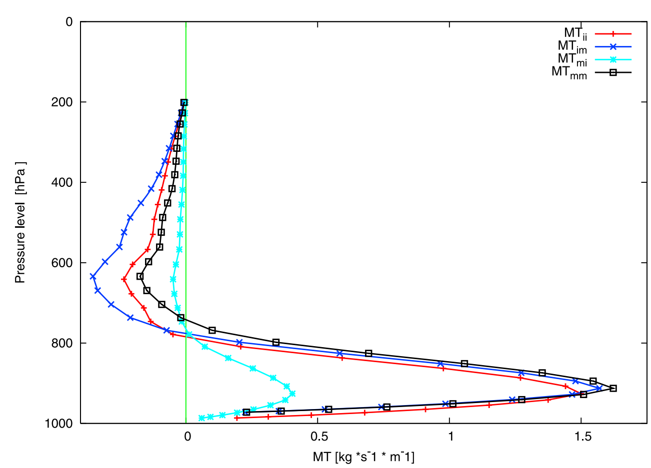

Figure 5. Vertical profiles of horizontal moisture transports per level. Magnitude of horizontal net moisture transport per model level along boundary of ASC. Positive (negative) values denote net transports into (out of) ASC. Symbols denote locations of mean pressure and mean transports of the respective 31 used model levels.

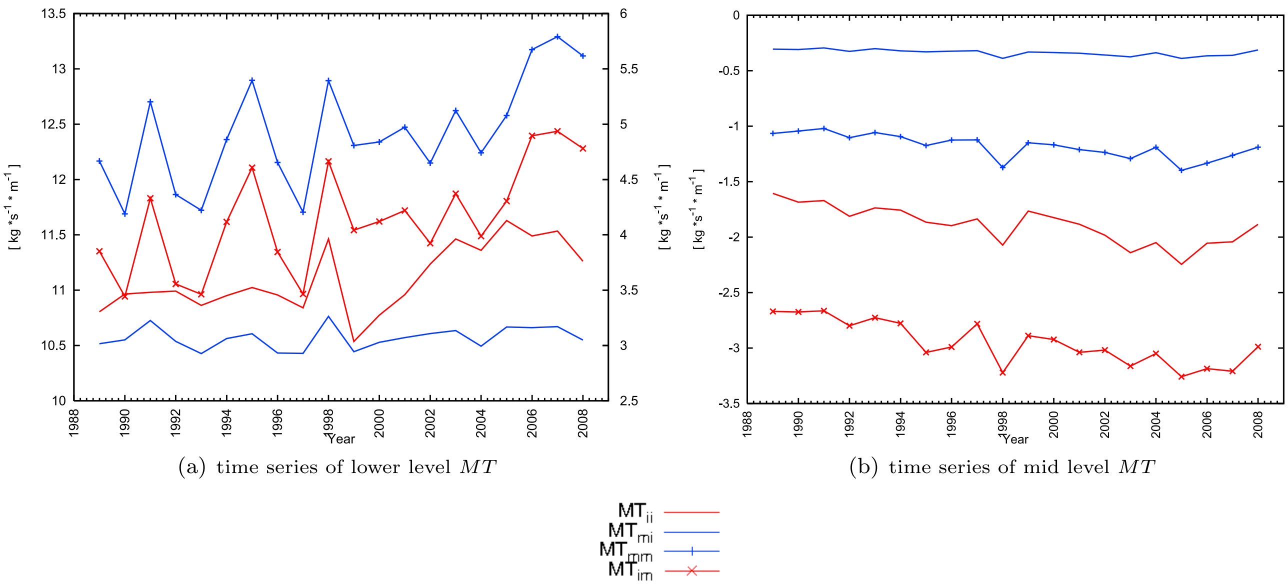

(a) time series of lower level MT

(b) time series of mid level MT

Figure 6. Time series of moisture transports below and above the reversal level. (a) Time series of the yearly mean net moisture transport below the reversal level (level of zero moisture transport budget in Figure 5, positive below and negative above). MT in MT_{mi} (solid blue lines) refers to right y axis. (b) Time series of the yearly mean net moisture transport above the reversal level. Negative values denote transports outward of ASC.

outflow at the midlevels above a particular reversal level (RL). Consistent with the low mean values of MT_{mi} discussed in sections 4.1 and 4.2, its vertical profile is relatively indistinct, with low inflow and almost no outflow. In the other experiments, the familiar vertical pattern is more pronounced. From the ground up to a level somewhat above 800 hPa, there is a net moisture input into ASC. This inflow peaks at about 926 hPa in MT_{ii}, somewhat lower than in the two ASC_m experiments, which both peak at 913 hPa. Also, maximum inflow per m and s is a little bit lower in MT_{ii}. Despite these differences in detail, the curves of all three experiments are by and large similar in magnitude and shape below the RL.

[37] Above the reversal level the situation is different. Although maximum outflows are at about the same level (633 hPa), the strength of outward transport is weakest in MT_{mm}, 1.5 times stronger in MT_{ii}, and about 2.5 times stronger in MT_{im}, which uses the same region as MT_{mm}. We propose that these inaccuracies are caused by the use of mean variables for the moisture budget estimations at the midlevels. Along the boundaries, wind vectors can have a positive or negative sign (directed inward and outward of ASC). Higher values of midlevel humidity are found during pronounced convective situations, when high upward ω induces higher midlevel humidity and stronger outward directed winds at the same time. These situations are represented more accurately in the small and quickly changing area of ASC_i. When averaging humidity or wind, the temporal coincidence of high outward wind and high humidity are averaged out, causing the systematic bias in the transport budget estimations.

[38] When calculating the total transport budget, the lower-level positive and the midlevel negative net transport neutralize each other, at least to some extent. In MT_{mm}, where this counteracting of the midlevel outflow is represented insufficiently, the trend in the net moisture budget is statistically most significant. To more closely investigate the changes in the inflow and outflow, we subdivided the change in the moisture budget into two parts: the time series of the net moisture inflow at the lower levels (below RL) and the time series of the net moisture outflow at the midlevels (above RL).

[39] The temporal evolutions of both are found in Figure 6. Again, the unfeasibility of MT_{mi} becomes evident. Inflow and outflow are far too low, thus MT_{mi} will be omitted from the following discussion.

[40] Inflows are highest into ASC_m (lines with crosses). Here they are highest, when mean wind vectors and mean values for humidity are applied. Contrary to what the mean Hadley circulation pattern suggests, the direction of wind vectors may also be variable at the lower level and thus also frequently directed outward of ASC, at least in the instantaneous fields. If these are averaged out as done in MT_{mm}, this does artificially increase the total mean input. In the experiments using instantaneous variables, these outward transports are resolved, diminishing the lower-level budget.

[41] Nevertheless, all the lower-level inflows share increasing trends, which are statistically significant at high levels (Table 4). Coinciding with this increase in the lower-level inflow, the midlevel outflow is also strengthening. Their trends as calculated by a least squares fit are a bit lower in magnitude but are all significantly different at high levels. The strengthened outflow counteracts the increase in the inward directed transport but is weaker in magnitude. Note that the sum of the trend of inflow and outflow adds to the trend of the total net budget of moisture transport (Table 3). This counteracting of the trend in the outflow is most pronounced for the instantaneous variables in MT_{ii}, where its magnitude is $\sim\frac{2}{3}$ of the inflow's increase and is much less distinctive for MT_{mm} ($\sim\frac{1}{5}$ only).

Table 4. Statistical Values of Time Series of Lower-Level Net Moisture Inflow and Midlevel Net Moisture Outflow m[a]

Acronym	Mean (kg m^{-1} s^{-1}) In	Mean Out	σ (kg m^{-1} s^{-1}) In	σ Out	Trend ((kg m^{-1} s^{-1}) yr^{-1}) In	Trend Out	Significant Level of Trend In	Significant Level of Trend Out
MT_{ii}	11.10	-1.89	0.30	0.17	0.0336	-0.0226	s 0.99, ns 0.995	s 0.995
MT_{im}	11.65	-2.95	0.47	0.2	0.0509	-0.0272	s 0.995	s 0.995
MT_{mm}	12.42	-1.18	0.49	0.11	0.0507	-0.0140	s 0.975, ns 0.99	s 0.995
MT_{mi}	3.07	-0.34	0.1	0.03	0.0041	-0.0031	ns 0.9	s 0.995

[a]See Figure 6. Acronym, acronym of experiments; mean, average over investigation period (1989–2008); σ, standard deviation of annual means; trend, trend of annual mean (as calculated by a least squares fit); and significance level of trend, level at which trend is significant (s) and/or no longer significant (ns). Statistical significance is tested according to a t test based on the yearly numbers. In (out) denotes values for the flow below (above) the reversal level (see text).

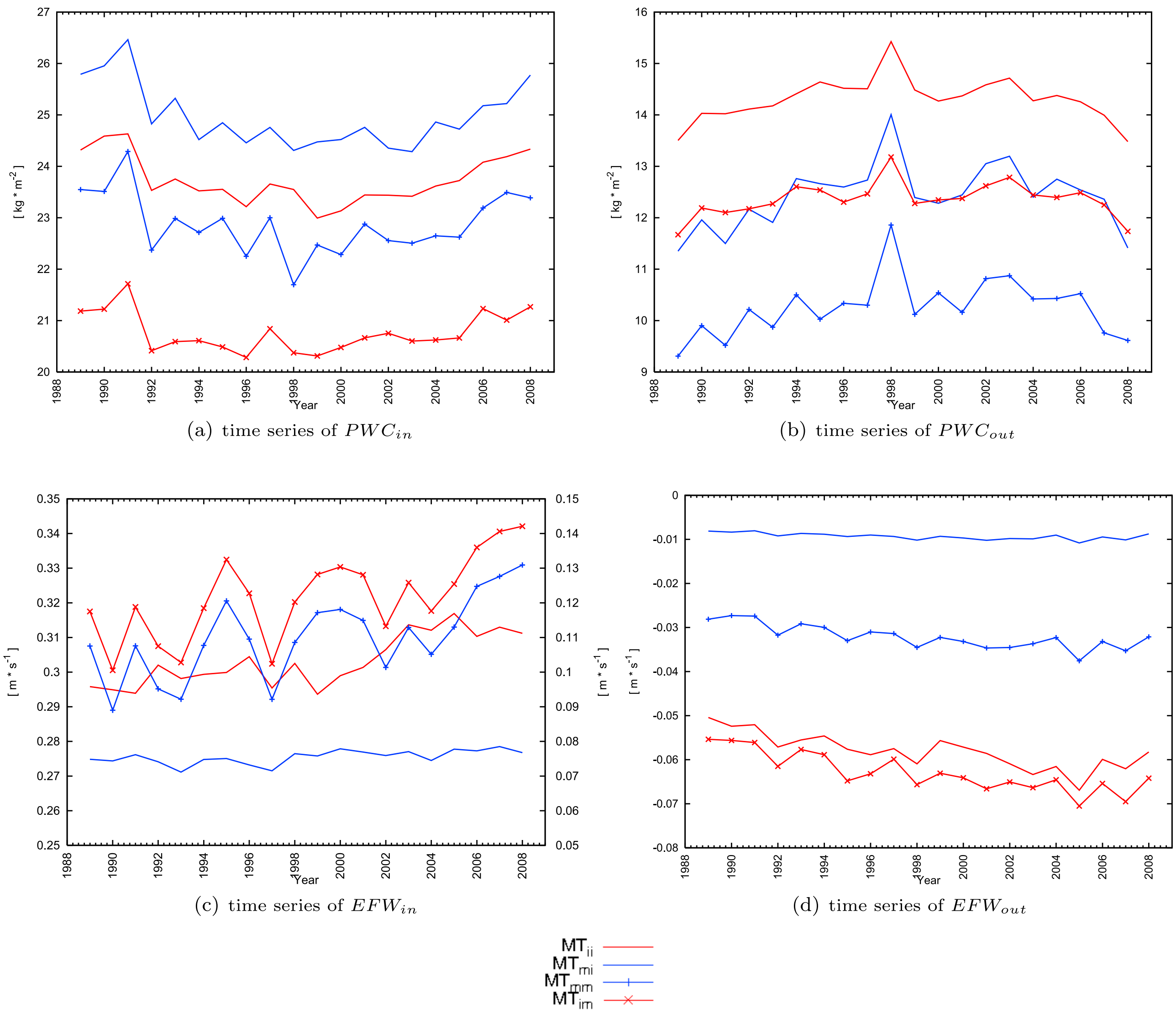

Figure 7. Water content (PWC) and effective wind (EFW) along boundary of ASC. (a and b) Time series of yearly mean PWC along the boundary of ASC below and above the reversal level (level of zero moisture transport budget in Figure 5). (c and d) Time series of yearly mean EFW along the boundary of ASC. Red (blue) lines indicate estimations based on instantaneous (monthly) mean wind and humidity. Solid (crossed) lines indicate ASC (DESC) mask based on instantaneous (monthly) mean ω. EFW is mean wind of layer weighted by fraction of PWC in that layer relative to PWC of total column [cf. *Sohn and Park*, 2010].

Table 5. Statistical Values of Time Series of Lower-Level and Midlevel Precipitable Water Content[a]

	Mean (kg m^{-2})		σ (kg m^{-2})		Trend ((kg m^{-2}) yr^{-1})		Significant Level of Trend	
Acronym	In	Out	In	Out	In	Out	In	Out
MT_{ii}	23.73	14.31	0.47	0.42	-0.012407	0.005182	ns 0.9	ns 0.9
MT_{im}	20.77	12.36	0.39	0.33	-0.002367	0.010631	ns 0.9	ns 0.9
MT_{mm}	22.87	10.25	0.61	0.56	-0.017624	0.025707	ns 0.9	s 0.9, ns 0.95
MT_{mi}	24.97	12.42	0.59	0.62	-0.032337	0.029766	ns 0.9	ns 0.9

[a]See Figure 7. Acronym, acronym of experiment; mean, average PWC over investigation period (1989–2008); σ, standard deviation of annual means; trend, trend of annual mean (as calculated by a least squares fit); and significance level of trend, level at which trend is significant (s) and/or no longer significant (ns). Statistical significance is tested according to a *t* test based on the yearly numbers. In (out) denotes values for the flow below (above) the reversal level (see text).

[42] We conclude that there has been an increase in tropical moisture transports over the past 20 years, which affected both the inflow as well as the outflow. Because inflow and outflow are counteracting each other to some extent, a trend in the total net moisture budget is not significant. As the midlevel outflow is not represented well when looking at mean values or when using transports at a particular level as a proxy, this trend in the net budget may appear stronger as it is.

[43] This picture is improved when transports are calculated on the basis of instantaneous values, which do resolve the inflow and the outflow. Then it becomes evident that transports within the tropics have a more pronounced intensification than predicted from the mean values only. We find a statistically significant increase at the lower level as well as at the midlevel, even over a relatively short period of 20 years. The signal of a change in the net budget has a less-pronounced increase because the increase of the inflow was to some extent neutralized by the strengthening of the outflow.

4.4. Changing Atmospheric Water Content and Wind

[44] An increase in water vapor transport may be induced by increasing atmospheric humidity or by an intensification of the atmospheric wind circulation (e.g., *Held and Soden* [2006]. Here we will break down changes in the transport into ASC into changes in humidity and in wind circulation individually. Consistent with our moisture transport calculation (equation (1)), humidity is looked at using PWC_{bl}, summarized above the reversal level on the one hand and summarized below on the other. For the wind we use a humidity-independent measure, the so-called effective wind (EFW) as introduced by *Sohn and Park* [2010]. They remove the influence of water vapor changes by weighting the wind vector at a vertical level with the fraction of corresponding total water vapor. *Sohn and Park* [2010] found a significant strengthening in EFW over our time period on the lower layers and a minor strengthening at the midlevels. They derive the EFW from coarser-resolution reanalyses [*Sohn and Park*, 2010, Figure 2d] and for the December–February period averaged over the 30°N–15°S latitudinal band. As for PWC, we averaged the orthogonal component of the wind vector along the boundary separating ASC and DESC, across all levels above the reversal level on the one hand and below the reversal level on the other. Both were multiplied by the corresponding fraction of PWC, resulting in the EFW for the lower-level inflow and for the midlevel outflow over the entire tropics. The time series of their yearly means are shown in Figure 7.

[45] The trends in the time series of PWC above and below the RL are insignificant. Below the RL along the boundary of ASC, there are high values in the beginning and in the end of the time period and lower ones in between. Overall we find a slight downward trend, however not statistically significant, and thus not in conflict with an expected increase in PWC as a response to atmospheric warming. The situation is reversed on the midlevels, with lower values in the beginning and end and higher ones in between. In the El Niño year 1998, a pronounced peak is visible. Again trends are statistically insignificant or significant on a low level only Table 5 and 6.

[46] Total PWC values are highest for instantaneous values along ASC_i, especially at the midlevels. This may reflect the temporal coincidence of strong ω and midlevel humidity in the better-resolved convective tropical cells, with particularly warm temperatures, higher water-holding capacities, and stronger upward ω, ingesting the moisture and lifting it up to the midparts of the atmosphere.

Table 6. Statistical Values of Time Series of Lower-Level and Midlevel Effective Wind[a]

	Mean (m s^{-1})		σ (m s^{-1})		Trend ((m s^{-1}) yr^{-1})		Significant Level of Trend	
Acronym	In	Out	In	Out	In	Out	In	Out
MT_{ii}	0.303	-0.0581	0.007383	0.004028	0.001018	-0.000540	s 0.995	s 0.995
MT_{im}	0.322	-0.0629	0.012115	0.004387	0.001393	-0.000626	s 0.995	s 0.995
MT_{mm}	0.31	-0.0321	0.011813	0.002713	0.001322	-0.000356	s 0.995	s 0.995
MT_{mi}	0.076	-0.0093	0.002003	0.000736	0.000204	-0.000081	s 0.995	s 0.995

[a]See Figure 7. Acronym, acronym of experiment; mean, average EFW over investigation periods (1989–2008); σ, standard deviation of annual means; trend, trend of annual mean (as calculated by a least squares fit); and significance level of trend, level at which trend is significant (s) and/or no longer significant (ns). Statistical significance is tested according to a *t* test based on the yearly numbers. In (out) denotes the values for the flow below (above) the reversal level (see text).

[47] We can confirm the strengthening of EFW as demonstrated by *Sohn and Park* [2010] at the lower levels. A distinct and statistically significant increase is found in all of our experiments. However, we also find changes at the higher levels, which are highly significant in all experiments. In accordance with our previous findings for ASC_m, the inward directed trends have a magnitude similar to the instantaneous and mean humidity and wind experiment, but at the midlevels, the trend is only half as pronounced in the experiment applying mean humidity and winds, supporting our assumption that situations of high outward transport are averaged out in MT_{mm}.

5. Summary and Conclusion

[48] We have calculated moisture transports from tropical regions of descending air motion (DESC) into regions of tropical updraft (ASC) in four different experiments, all on the basis of the high space and time resolution reanalyses data of ERA-Interim. As conducted in several other studies, ASC and DESC are estimated from vertical winds on the basis of temporal average values over a month. We think that this averaged view is insufficient for a detailed picture of moisture transports in the tropics. We additionally defined ASC on the basis of instantaneous vertical wind, which at the high resolution of ERA-Interim allows for a much better representation of the very irregular pattern of numerous individual convective cells and regions over the tropics rather than a "single" zone extending all along the equator, the more conventional depiction of the Hadley Cell.

[49] For both ASC masks, we calculated the moisture transports across the boundary dividing ASC and DESC. Again we use monthly averaged variables and instantaneous ones.

[50] Our results do not contradict but rather modify knowledge gained from previous average value-based studies:

[51] 1. The increase in the moisture budget suggested by studies solely applying mean values seems to be too high, as the midlevel outflows are underestimated. If instantaneous values are applied, the moisture budget's increase is lower.

[52] 2. We found an underrepresentation of the midlevel outflow when using mean values. We suggest that this underrepresentation is the reason for the higher increase in the mean value-based moisture budget. Using instantaneous values, lower-level inflow and midlevel outflow neutralize each other to a greater extent.

[53] 3. If the changes in the lower-level inflow and the midlevel outflow are looked at individually, a strong significant increase is found in both, suggesting a strengthening of tropical circulation over the past 20 years. A slightly higher increase in the net inward transport results in weakening of ASC according to the literature (e.g., *Wentz et al.* [2007] and *John et al.* [2009]).

[54] We conclude that changes in the statistical properties may be estimated correctly in sign by using average values or proxies (e.g., conditions at the 850 hPa level). In many cases there is no alternative, especially if satellite data are applied, which usually do not contain any vertically resolved information. However, a more realistic quantitative assessment requires more highly resolved information. Our approach can easily be applied to model data, i.e., to estimate changes in IPCC future projections or in sensitivity studies.

[55] **Acknowledgments.** The authors would like to thank ECMWF for making the ERA-Interim data available. M.Z. was funded by the NERC PREPARE project, NE/G015708/1.

References

Allan, R. P., and B. J. Soden (2007), Large discrepancy between observed and simulated precipitation trends in the ascending and descending branches of the tropical circulation, *Geophys. Res. Lett.*, *34*, L18705, doi:10.1029/2007GL031460.

Allan, R. P., and B. J. Soden (2008), Atmospheric warming and the amplification of precipitation extremes, *Science*, *321*, 1481–1484.

Allan, R. P., B. J. Soden, V. O. John, W. Ingram, and P. Good (2010), Current changes in tropical precipitation, *Environ. Res. Lett.*, *5*, 025205, doi:10.1088/1748-9326/5/2/025205.

Allen, M. R., and W. J. Ingram (2002), Constraints on future changes in climate and the hydrologic cycle, *Nature*, *419*, 224–232.

Bengtsson, L., K. I. Hodges, S. Koumoutsaris, M. Zahn, and N. Keenlyside (2011), The changing atmospheric water cycle of the polar regions in a warmer climate, *Tellus, Ser. A*, doi:10.1111/j.1600-0870.2011.00534.x.

Bigg, G. R. (2006), Comparison of coastal wind and pressure trends over the tropical Atlantic: 1946–1987, *Int. J. Climatol.*, *13*, 411–421.

Chou, C., J.-Y. Tu, and P.-H. Tan (2007), Asymmetry of tropical precipitation change under global warming, *Geophys. Res. Lett.*, *34*, L17708, doi:10.1029/2007GL030327.

Dee, D. P., and S. Uppala (2009), Variational bias correction of satellite radiance data in the ERA-Interim reanalysis, *Q. J. R. Meteorol. Soc.*, *135*, 1830–1841.

Dee, D. P., et al. (2011), The ERA-Interim reanalysis: Configuration and performance of the data assimilation system, *Q. J. R. Meteorol. Soc.*, *137*, 553–597.

Gastineau, G., and B. J. Soden (2011), Evidence for a weakening of tropical surface wind extremes in response to atmospheric warming, *Geophys. Res. Lett.*, *38*, L09706, doi:10.1029/2011GL047138.

Harrison, D. E. (1989), Post–World War II trends in tropical Pacific surface trades, *J. Clim.*, *2*, 1561–1563.

Held, I. M., and B. J. Soden (2006), Robust responses of the hydrological cycle to global warming, *J. Clim.*, *19*, 5686–5699.

John, V. O., R. P. Allan, and B. J. Soden (2009), How robust are observed and simulated precipitation responses to tropical ocean warming?, *Geophys. Res. Lett.*, *36*, L14702, doi:10.1029/2009GL038276.

Kalnay, E., et al. (1996), The NCEP/NCAR reanalysis project, *Bull. Am. Meteorol. Soc.*, *77*, 437–471.

Lu, J., G. A. Vecchi, and T. Reichler (2007), Expansion of the Hadley cell under global warming, *Geophys. Res. Lett.*, *34*, L06805, doi:10.1029/2006GL028443.

Mitas, C. M., and A. Clement (2005), Has the Hadley cell been strengthening in recent decades?, *Geophys. Res. Lett.*, *32*, L03809, doi:10.1029/2004GL021765.

O'Gorman, P. A., and C. J. Muller (2010), How closely do changes in surface and column water vapor follow Clausius-Clapeyron scaling in climate change simulations?, *Environ. Res. Lett.*, *5*, 025207, doi:10.1088/1748-9326/5/2/025207.

Power, S. B., and I. N. Smith (2007), Weakening of the Walker Circulation and apparent dominance of El Niño both reach record levels, but has ENSO really changed?, *Geophys. Res. Lett.*, *34* (18), L18702, doi:10.1029/2007GL030854.

Seager, R., N. Naik, and G. A. Vecchi (2010), Thermodynamic and dynamic mechanisms for large-scale changes in the hydrological cycle in response to global warming, *J. Clim.*, *23*, 4651–4668.

Simmons, A., S. Uppala, D. Dee, and S. Kobayashi (2007), Era-Interim: New ECMWF reanalysis products from 1989 onwards, *ECMWF Newsl. 110*, pp. 25–35, Eur. Centre for Medium-Range Weather Forecasts, Reading, U. K.

Sohn, B. J., and S.-C. Park (2010), Strengthened tropical circulations in past three decades inferred from water vapor transport, *J. Geophys. Res.*, *115*, D15112, doi:10.1029/2009JD013713.

Sohn, B.-J., E. A. Smith, F. R. Robertson, and S.-C. Park (2004), Derived over-ocean water vapor transports from satellite-retrieved $E - P$ datasets, *J. Clim.*, *17*, 1352–1365.

Trenberth, K. E., A. Dai, R. M. Rasmussen, and D. B. Parsons (2003), The changing character of precipitation, *Bull. Am. Meteorol. Soc.*, *84*, 1205–1217.

Trenberth, K. E., J. Fasullo, and L. Smith (2005), Trends and variability in column-integrated atmospheric water vapor, *Clim. Dyn.*, *24*, 741–758, doi:10.1007/s00382-005-0017-4.

Uppala, S. M., et al. (2005), The ERA-40 reanalysis, *Q. J. R. Meteorol. Soc.*, *131*, 2961–3012.

Vecchi, G. A., B. J. Soden, A. T. Wittenberg, I. M. Held, A. Leetmaa, and M. J. Harrison (2006), Weakening of tropical Pacific atmospheric circulation due to anthropogenic forcing, *Nature*, *441*, 73–76.

Wentz, F. J., and M. Schabel (2000), Precise climate monitoring using complementary satellite data sets, *Nature*, *403*, 414–416.

Wentz, F. J., L. Ricciardulli, K. Hilburn, and C. Mears (2007), How much more rain will global warming bring?, *Science*, *317*, 233–235.

Whysall, K. D. B., N. S. Cooper, and G. R. Bigg (1987), Long-term changes in the tropical Pacific surface wind field, *Nature*, *327*, 216–219.

R. P. Allan, Department of Meteorology, University of Reading, Earley Gate, PO Box 243, Reading RG6 6AL, UK.

M. Zahn, Environmental Systems Science Centre, University of Reading, Harry Pitt Building, 3 Earley Gate, Whiteknights, Reading RG6 6AL, UK. (m.zahn@reading.ac.uk)